DTU Library

Primary Paralleled Isolated Boost Converter with Extended Operating Voltage Range

Hernandez Botella, Juan Carlos; Sen, Gökhan; Mira Albert, Maria del Carmen; Thomsen, Ole Cornelius; Andersen, Michael A. E.

[Link back to DTU Orbit](#)

Primary Paralleled Isolated Boost Converter with Extended Operating Voltage Range

Juan C. Hernandez B.,Gokhan Sen, Maria C. Mira A., Ole C. Thomsen, Michael A. E. Andersen

Technical University of Denmark, Ørsteds Plads, 349. Kgs. Lyngby, Denmark

s101905@student.dtu.dk, gs@elektro.dtu.dk, s101901@student.dtu.dk, oct@elektro.dtu.dk, ma@elektro.dtu.dk

Abstract

Applications requiring wide input and output voltage range cannot often be satisfied by using buck or boost derived topologies. Primary paralleled isolated boost converter (PPIBC) [1]-[2] is a high efficiency boost derived topology. This paper proposes a new operation mode for extending the input and output voltage range in PPIBC. The proposed solution does not modify PPIBC power stage, the converter gain is modified instead by short circuiting one of the paralleled connected primary windings present in this topology.

Keywords: Isolated boost, battery, extended range.

Nomenclature:

R_g	Source series resistance
V_g	Source voltage
$R_{D_{Bat}}$	Battery dynamic resistance
$V_{OC_{Bat}}$	Battery open circuit voltage
r_L	Inductor parasitic resistance
r_{MP}	Primary MOSFET's on resistance
r_p	Transformer primary resistance
r_S	Transformer secondary resistance
r_{MS}	Secondary MOSFET's on resistance

1. Introduction

In this paper an alternative solution with an extended voltage operation range is proposed based on modifying the operating mode of PPIBC, which has been reported [1]-[2] as a high efficient solution in low voltage high current applications. This topology, derived from the simple isolated boost converter, increases the efficiency by splitting the primary current through two parallel primary stages (Figure 1). This approach results in reduced ac current loops which helps reducing the power stage layout stray inductances. Together with the transformer leakage inductances, stray inductances increase the switching loses. In addition, the two transformer secondary windings are connected in series which reduces the number of turns on the secondary side for individual transformers allowing for an easier magnetic component design. The primary switches in each parallel stage are driven with identical gate signals. Moreover, the two stages share the input inductor as well as the input and output filters, which makes this topology a simpler solution. Due to the transformer series connection on the secondary side the two currents flowing through the two primary stages are forced to be equal during the inductor discharge state. In order to balance the current between the primary stages a current balancing transformer (CBT) [3] is inserted. This component is implemented as two inversely coupled inductors that present high impedance in case of current imbalance, keeping the current in each parallel stage equal. The converter schematic and steady state operating waveforms are presented in (Figure 1). The voltage gain is given in (1).
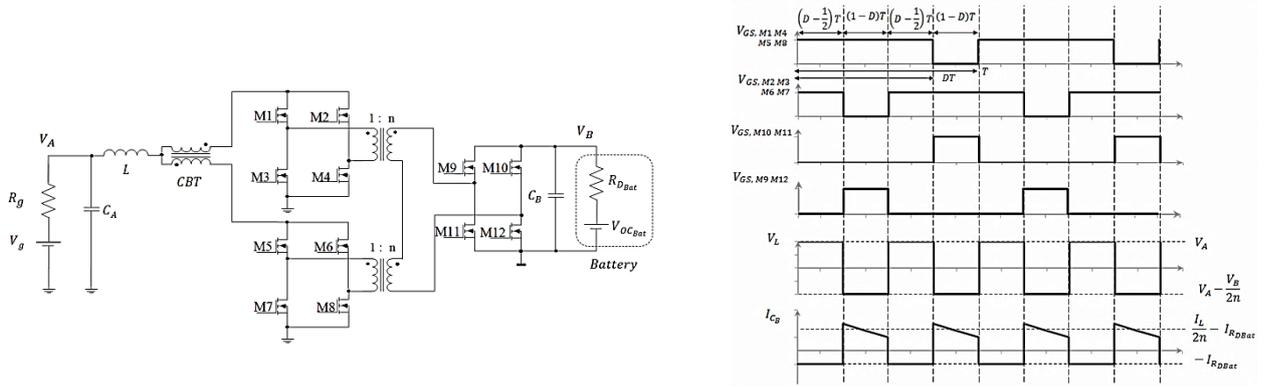
Figure 1. PPIBC schematic and steady state waveforms

$$M(D) = \frac{V_B}{V_A} = n \cdot \frac{1}{(1 - D)} \tag{1}$$

Boost derived topologies can ideally increase their output voltages up to very high values when the primary switches' duty cycle approaches 100%. Therefore it is possible to adjust the turn ratio of the transformer such that the full operating range can be covered by adjusting the duty cycle. However, operating the converter with extreme duty cycles will significantly increase the rms current stress in the components, which will affect the converter efficiency. Therefore, a change in converter operation mode could be utilized to keep the switch duty cycles in acceptable values.

2. Extended operating voltage range

The state-of-the art solution for extended voltage range in isolated boost converters has been presented in the literature [4]-[5]. The solution in [4] proposes an auxiliary winding in the input inductor that will provide flyback operation to the converter, extending the operating voltage range and solving the intrinsic start up problems in boost derived topologies. However, this is not an efficient solution in high power applications and makes the manufacturing process of the input inductor more complicated because extensive interleaving techniques will have to be adopted to increase the coupling coefficient of the flyback winding.

This paper presents an efficient solution for extending the voltage range of PPIBC by implementing a new operation mode where the two upper side MOSFETs in one of the parallel stages are shut down while the lower side switches are kept in conduction mode. This new operation mode effectively reduces the equivalent converter conversion ratio by short circuiting the primary winding in one of the primary stages which deactivates the corresponding transformer. As in the auxiliary flyback winding configuration, the main drawback of this solution is the increased voltage stress on the primary switches during extended operation (2). This fact will increase the requirement for the primary switch breakdown voltage, consequently increasing the device on resistance which affects the converter efficiency.

$$V_{DS_{PPIBC}} = \frac{V_B}{2 \cdot n} \qquad V_{DS_{Flyback}} = V_A + \frac{V_B}{2 \cdot n} \qquad V_{DS_{PPIBC\_Extended}} = \frac{V_B}{n} \tag{2}$$

However this is an attractive solution in applications with variable output voltage where the extended mode will be operated only under minimum output voltage. For example in battery applications when a heavy load condition is applied to the battery, the battery voltage will collapse (acceleration event in an electric vehicle). (Figure 2) and (Figure 3) present the converter steady state waveforms and voltage gain during extended voltage range operation. (3) gives the modified voltage conversion ratio.
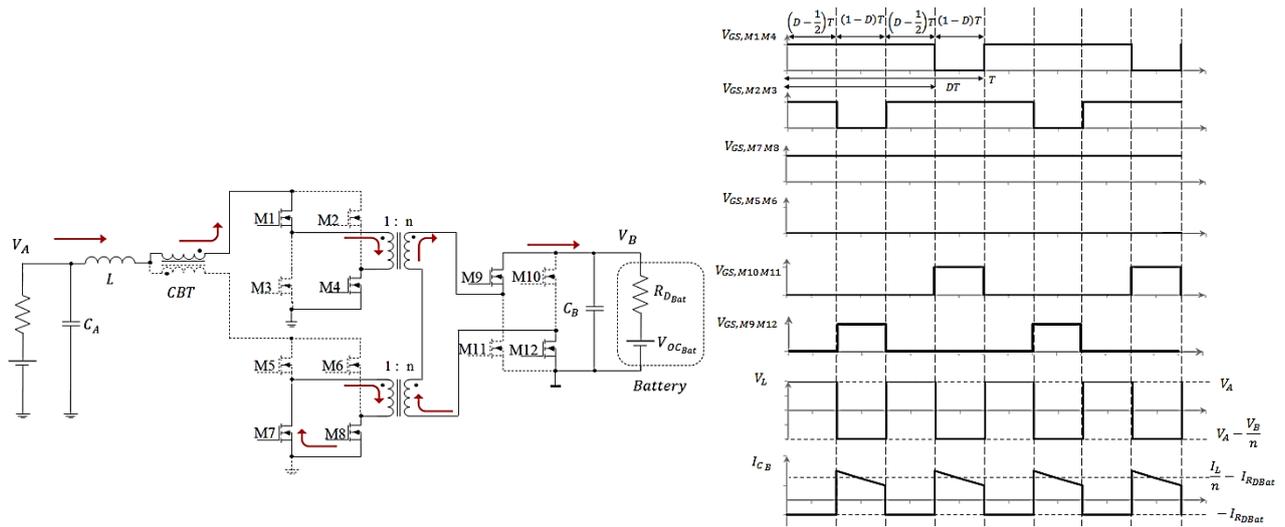
2

Figure 2. PPIBC steady state waveforms during extended voltage operation

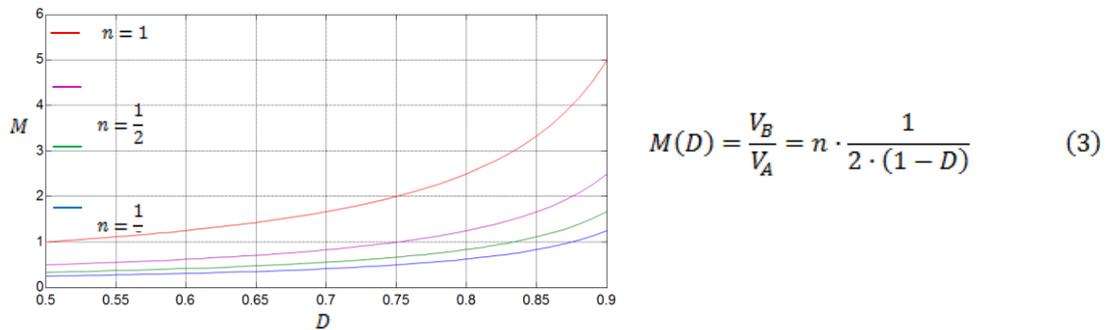$$M(D) = \frac{V_B}{V_A} = n \cdot \frac{1}{2 \cdot (1 - D)} \qquad (3)$$

Figure 3. Converter voltage gain during extended operation mode for different transformer turns ratios

3. Simulation of PPIBC with extended voltage range operation

The proposed solution is analyzed by performing several LTspice simulations with the operating conditions shown in Table 1. (Figure 4) presents a simulation result where the inductor current level is fixed at $20A$ during closed loop operation of the converter. It can be observed that during the transition the current deviates from the reference value until the loop is able to compensate the error. The deviation in the current during the transition is caused by the change in the converter steady state conditions and the sensitivity of the inductor current to duty cycle perturbations as shown in [6]. This will increase the components' current stress which reduces the converter reliability.

Table 1 Parameters of the converter

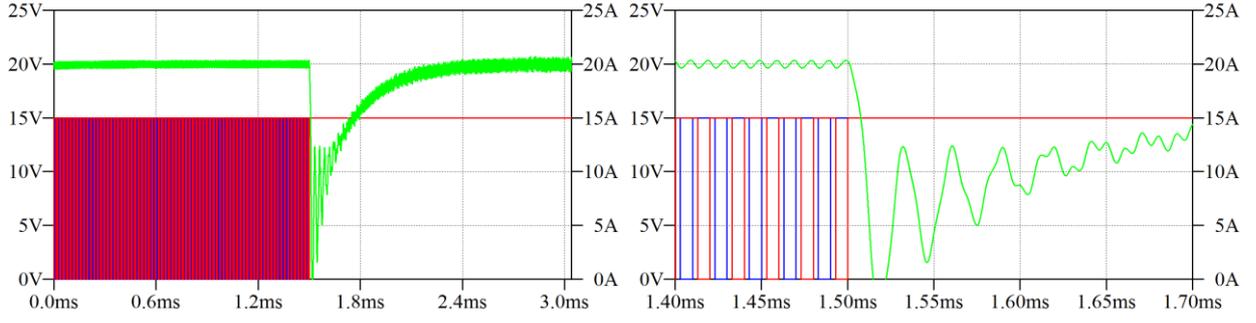|	
Source voltage	30 V
Battery terminal voltage	24 V
Transformer turn ratio	3 : 1
Inductor	13.5 µH
Capacitor A	40 µF
Capacitor B	120 µF
Switching frequency	50 kHz
Source output resistance	10 mΩ
Battery dynamic resistance	60 mΩ

Figure 4. Simulated transition from normal operation mode to extended operation mode (left) and detailed zoomed of the transition (right). Converter input current I_g (green), M1 and M3 gate signal (red and blue).

4. Transition with pre-calculated steady-state duty cycle

The current stress during transition time can be reduced if a steady state duty cycle pre-calculation is performed based on an accurately derived model of the converter. In battery loading applications, as presented in [6]-[7], the duty cycle-to-inductor current transfer function is heavily affected by the converter parasitic resistances due to the low value of the battery dynamic resistance. (Figure 6) present the inductor charging and discharging states during extended voltage range operation.
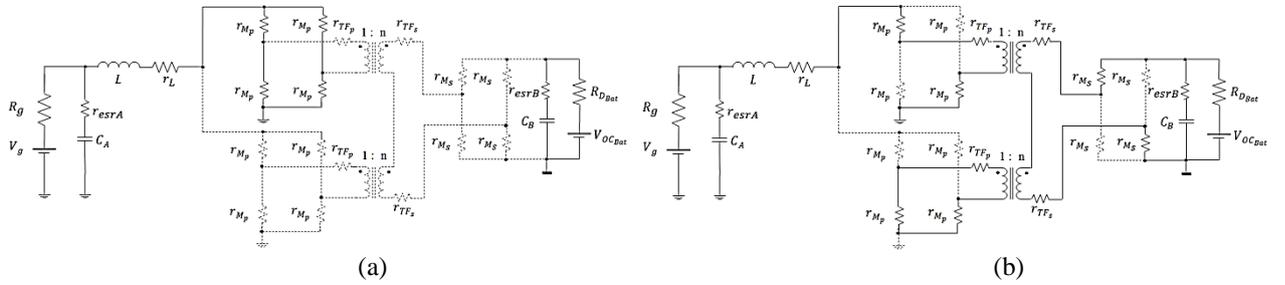

(a)   (b)

Figure 6. PPIBC conduction states during extended voltage range operation. (a) inductor charging subinterval, (b) inductor discharging subinterval

Based on the conduction states in (Figure 6) a new model can be obtained for the extended operating voltage mode. In this way, the converter duty cycle can be calculated prior to the transition between operating modes by using (4).

$$D = 2 \cdot \left(1 - \frac{I_L \cdot \left(R_g + \frac{R_{D_{Bat}}}{N_e^2} + r_{eq2} \right) + \frac{V_{OC_{Bat}}}{N_e} - V_g}{I_L \cdot \left(\frac{R_{D_{Bat}}}{N_e^2} + r_{eq2} - r_{eq1} \right) + \frac{V_{OC_{Bat}}}{N_e}} \right) \tag{4}$$

Where N_e corresponds to the effective transformer ratio and equivalent resistances r_{eq1} and r_{eq2} are defined as shown in (5) for normal operating mode and (6) for extended operating mode.

$$N_e = 2 \cdot n \qquad r_{eq1} = r_L + r_{M_P}/2 \qquad r_{eq2} = r_L + r_{M_P} + \frac{r_P}{2} + \frac{2r_S}{(2n)^2} + \frac{2r_{M_S}}{(2n)^2} \tag{5}$$

$$N_e = n \qquad r_{eq1} = r_L + r_{M_P} \qquad r_{eq2} = r_L + 4r_{M_P} + 2r_P + \frac{2r_S}{n^2} + \frac{2r_{M_S}}{n^2} \tag{6}$$

(Figure 7) shows a mode transition event where the controller has been set to produce the pre-calculated duty cycle before the transition event between operating modes.
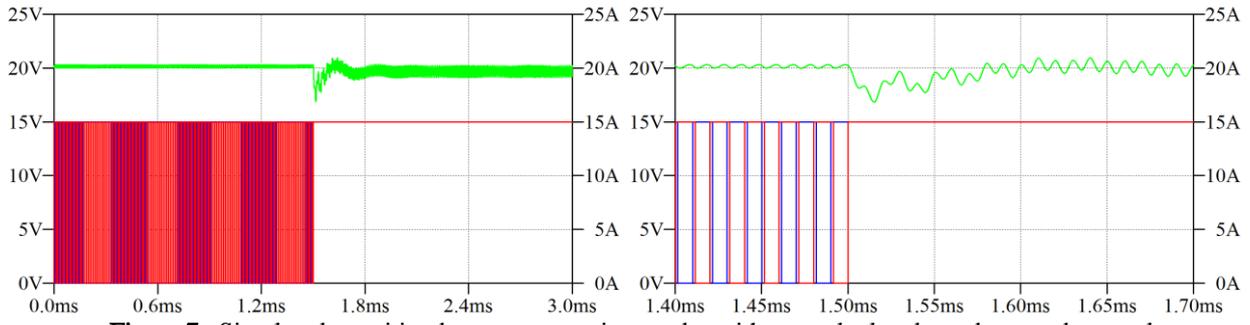
4

Figure 7. Simulated transition between operating modes with pre-calculated steady state duty cycle

4. Experimental results

A DSP controlled PPIBC has been used to experimentally verify the operation of the converter in extended mode. The gate signals in one of the paralleled primary stages have been modified by inserting some control logic circuitry to produce the desired waveforms under extended operation mode. The implemented prototype and the gate drive circuitry are shown in (Figure 8) and (Figure 9) respectively.
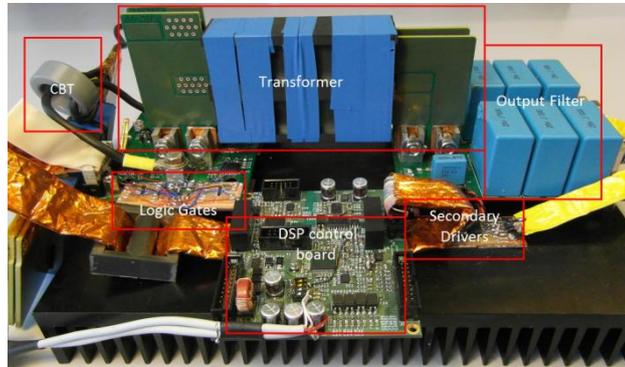

Figure 8. Experimental prototype

(a)   (b)
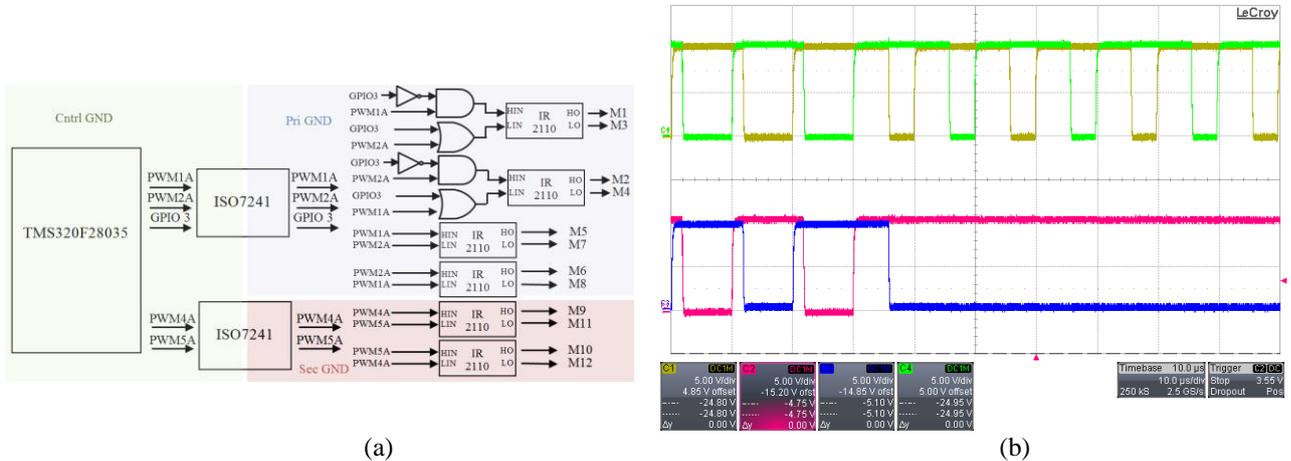
Figure 9. Gate drive circuitry (a) and gate waveforms during normal to extended operating mode transition (b).

(Figure 10) shows a transition event from normal to extended operating mode with pre-calculated duty cycle during converter closed loop operation for an inductor current level equal to 20 A. The change in duty cycle and voltage stress can be observed on one of the primary MOSFETs drain to source voltage waveform. It can be noticed that during extended operation mode the voltage ringing during MOSFET off state increases respect the normal operation mode due to the effect of the leakage inductance of the short circuited transformer.
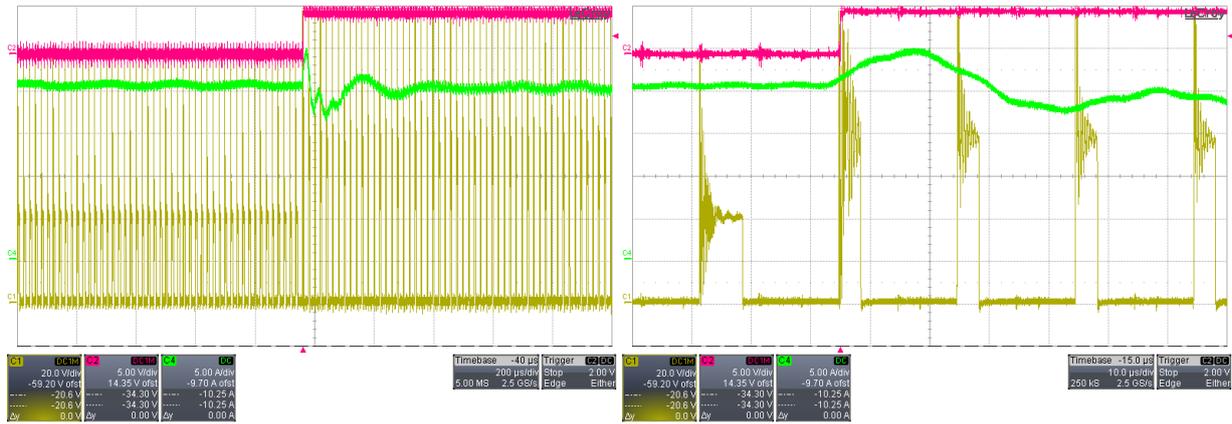
Figure 10. Transition between operating modes with pre-calculated steady state duty cycle (left, time scale: 200μs/div) and detailed zoomed of the transition (right, time scale:10μs/div). Source output current I_g (green, 5A/div), primary MOSFET drain to source voltage (brown, 20V/div) and short circuit control signal GPIO3 (red, 5V/div).

5. Conclusions

In applications requiring wide operating voltage ranges, extreme duty cycles and extreme turn ratios for transformers have to be selected for covering the converter specifications which will affect the converter efficiency. Optimizing the converter design for the most probable operating conditions and still covering all the possible operating points is desired. In order to do this a new method for extending the operating voltage range has been proposed for PPIBC where the effective converter voltage conversion ratio is changed by deactivating one of the transformers through short-circuiting its primary windings. This new operation mode has been tested in a series of simulations and experiments where it has been observed that the transition between normal and extended operating modes is a disturbance to the converter due to the change in steady state operating conditions. However, a very smooth transition can be obtained if the steady state duty cycle is pre-calculated based on an accurate model of the converter.

References

[1] M. Nymand and M. A. E. Andersen, "New primary-parallel boost converter for high-power high-gain applications" in Proc. IEEE APEC 2009, pp. 35-39.

[2] M. Nymand and M. A. E. Andersen, "A New Approach to High Efficiency in Isolated Boost Converters for High-Power Low-Voltage Fuel Cell Applications," Proc. EPE-PEMC, Poznan, Poland, 2008.

[3] Gokhan Sen , S. M. Dehghan, Ole C. Thomsen and Michael A. E. Andersen, "Comparison of Current Balancing Configurations for Primary Parallel Isolated Boost Converter," Acemp - Electromotion , 2011.

[4] L. Zhu, K. Wang, F. C. Lee, and J.-S. Lai., "New start-up schemes for isolated full-bridge boost converters," IEEE Trans. on Power Electron.,vol. 18, pp. 946–951, 2003.

[5] Kristian Lindberg-Poulsen, Ziwei Ouyang, Gokhan Sen, Michael A.E. Andersen, "A new method for start-up of isolated boost converters using magnetic- and winding-integration" APEC 2012, pp.340-345.

[6] Maria C. Mira A., Juan C. Hernandez B., Gokhan Sen, Ole C. Thomsen, Michael A.E. Andersen, "Modeling and Control of Primary Parallel Isolated Boost Converter" IECON 2012.

[7] Juan C. Hernandez B.,Maria C. Mira A., Gokhan Sen, Ole C. Thomsen, Michael A.E. Andersen, "Primary Parallel Isolated Boost Converter with Bidirectional Operation" VPPC 2012.